# Electronic structure and charge distribution of potassium iodide intercalated single-walled carbon nanotubes

ChiYung Yam, ChiChiu Ma, XiuJun Wang, and GuanHua Chen[a)]
*Department of Chemistry, The University of Hong Kong, Hong Kong, People's Republic of China*

(Received 10 May 2004; accepted 14 September 2004)

Recently, potassium iodide was inserted into single-walled carbon nanotubes. We present here a first-principles density-functional theory calculation of the electronic and optical properties of a potassium iodide intercalated (10,10) nanotube. Band structure, density of states, and charge distribution of the intercalated nanotube are determined. Significant changes in the electronic structure of carbon nanotube are found upon the intercalation. In particular, the electron distribution on the tube becomes more diffusive, and one out of every four K 4*s* electrons transfers to the tube wall, while the other three go to I 5*p* orbitals. © *2004 American Institute of Physics*.
[DOI: 10.1063/1.1819510]

Carbon nanotubes (CNTs)[1] have been a focus of research interest partly because of their rich electronic properties,[2,3] which may be tuned. Through physical or chemical modifications of the tubes, these physical properties can be further modified. Significant progress has been made in filling nanotubes with a range of materials.[4,5] A large enhancement in conductivity is reported by doping CNTs with potassium and bromine separately.[4,6] Experiment[5] and theoretical works[7] showed that CNTs can encapsulate fullerenes. This so-called carbon peapod was found to be a metal with multicarriers distributed both along the tube and on the $C_{60}$ chain. These examples show that the electronic properties of CNTs can be modified through chemical doping.

Recently, K and I were inserted into a (10,10) single-walled CNT (SWNT).[8,9] Lattice distortions for KI were observed which were attributed to the difference in K:I coordination from the bulk crystal and the interaction between the KI chain and the tubule wall. The resulting KI/SWNT composite is a highly anisotropic one-dimensional structure, and its electronic and optical properties may alter with respect to both the bulk halide and the pure nanotube. In this work, we employ first-principles density-functional theory (DFT) to calculate the electronic structure of the KI intercalated (10,10) SWNT.

The electronic structure is calculated within the framework of DFT.[10] We employ WIEN97 software package,[11] which is based on the full-potential linearized augmented plane wave (LAPW) method. Perdew–Wang parametrization[12] of local density approximation is adopted for the exchange-correlation functional. In the LAPW method, the unit cell is divided into two types of regions: the atomic spheres centered at nuclear sites and the interstitial region between the nonoverlapping spheres. The wave function is expanded in terms of atomic wave functions within the atomic spheres, and in terms of plane waves in the interstitial region.

In our calculations we adopt the experimental structure of KI@(10,10) reported in Ref. 8. The structure is depicted in Fig. 1. The muffin-tin radii are set to 1.30, 2.61, and 3.50 a.u. for carbon, potassium and iodine, respectively. The lattice parameters of KI@(10,10) in our calculation are: $a=18$ Å, $b=18$ Å, and $c=7.384$ Å. Linear chains of K and I are put into each nanotube, and each unit cell contains $K_4I_4C_{120}$. Across the SWNT capillary, K and I are spaced at an interval of 4.0 Å, whereas along the capillary the spacing is 3.69 Å. The center-to-center distance between the nanotubes in the neighboring cells is 18 Å, which is found to be a large enough separation to prevent intertubule interaction. To achieve the self-consistency for the electronic structure calculations, we use one $k$ point in the irreducible part of the Brillouin zone. The chosen $k$ point is at the center of the zone, that is, $\Gamma$ point, and the calculation is considered to be completed when the energy variation at $\Gamma$ point from one iteration to the next does not exceed $10^{-5}$ Ry.

Electronic band structures for (10,10) and KI@(10,10) CNTs are given in Figs. 2(a) and 2(b), respectively. The cell used in the calculation for (10,10) CNT contains 120 carbon atoms, which is three times as many as those of (10,10) CNT unit cell. It is chosen to match with the unit cell of KI@(10,10) CNT, so that a direct comparison of the electronic structures between (10,10) and KI@(10,10) CNTs is possible. Both (10,10) SWNT and KI@(10,10) SWNT show

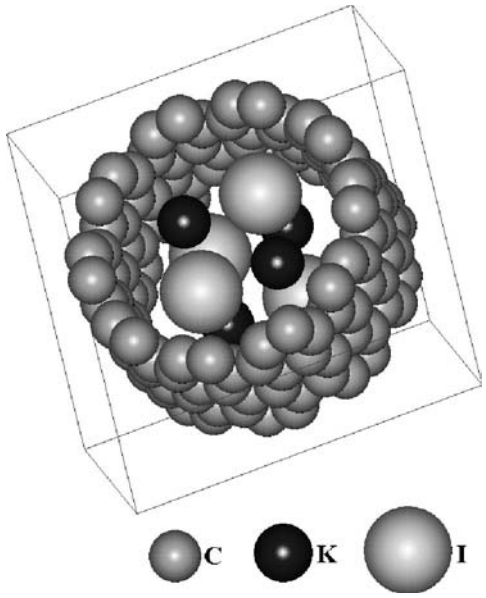


FIG. 1. Unit cell of a (10,10) CNT having potassium iodide inside.

[a)]Electronic mail: ghc@everest.hku.hk

 

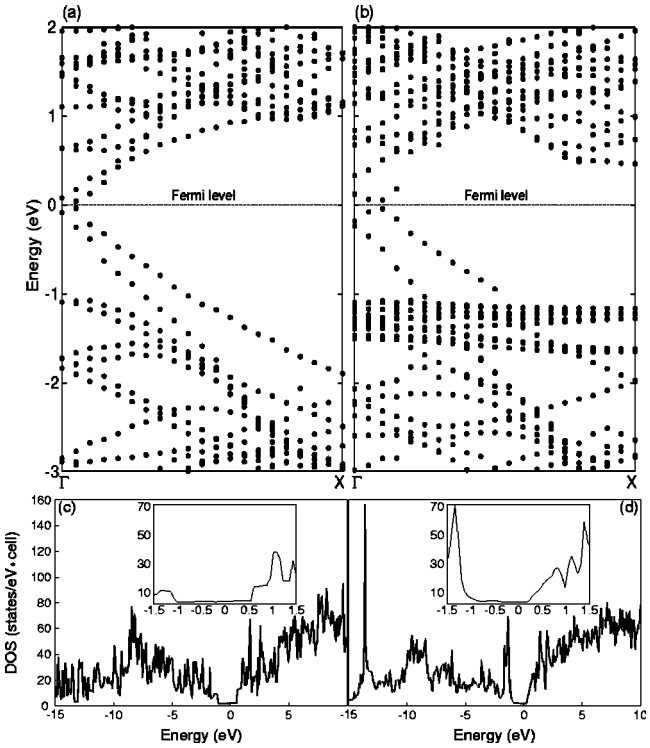


FIG. 2. (a) Band structure of (10,10) CNT. (b) Band structure of KI@(10,10). The Fermi level energy is set to 0 eV. $k=0$ at the $\Gamma$ point, and $k=\pi/3a_c$ at the $X$ point, where $a_c$ is the lattice parameter of the (10,10) CNT. (c) DOS for (10,10) CNT. (d) DOS for KI@(10,10) CNT.

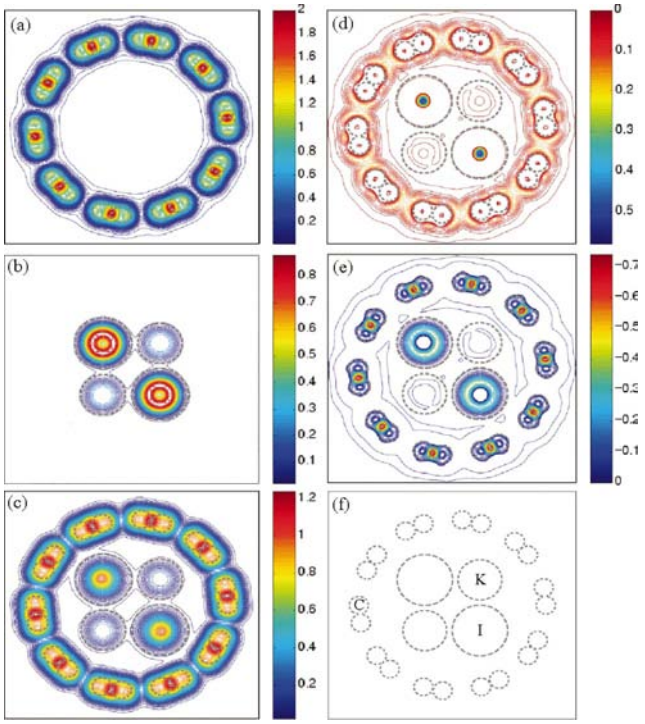


FIG. 3. (Color) Contour plots of the electron density (in electrons/Å$^3$) of (a) (10,10) CNT, (b) KI@(10,10), and (c) KI. We calculate the difference between the sum of electron densities of KI chain and (10,10) CNT and that of KI@(10,10) CNT. The increasing and decreasing portions of electron density are plotted in (d) and (e), respectively. (f) Division of unit cell. Regions encircled by gray dashed lines are the LAPW atomic spheres for carbon (C), potassium (K), and iodine (I). The remaining space is the LAPW interstitial region. The atomic spheres used in the calculations are also indicated in (a), (b), (c), (d), and (e).

metallic character. It is found that the flat bands at $\sim -1$ eV consist of I 5*p* orbitals, and the conduction bands between 1 and 2 eV in Fig. 2(b) contain large contributions from K 4*s* orbitals. The Fermi level intersects the electronic bands slightly off from the $\Gamma$ point in Fig. 2(a) for the (10,10) CNT (the X point here corresponds to the K point of graphite Brillouin zone). This is due to the hopping constants around the circumference and along the tube axis are slightly different. In Fig. 2(b), it is clearly shown that the intersect is further shifted for KI@(10,10) CNT. Moreover, the band structure near the Fermi level alters upon the KI intercalation although the metallic character is maintained. We plot the density of states (DOS) in Figs. 2(c) and 2(d). The insets in Figs. 2(c) and 2(d) show the DOS around the Fermi level. Clearly the DOS changes upon the KI intercalation, in particular, near the Fermi energy. The huge peak at −15 eV in Fig. 2(d) belongs to K 3*p* orbitals, and the peak at −1 eV in Fig. 2(d) corresponds mainly to the I 5*p* orbitals. Among other contributions, the broad band of peaks in Fig. 2(d) between 1 and 5 eV contains those from the K 4*s* orbital in addition to those of carbon atomic orbitals.

To further investigate the influence of the intercalation, we examine the electron distribution. Figures 3(a)–3(c) are the electron density contour plots for (10,10) CNT, KI chain, and KI@(10,10) CNT, respectively. Electron density becomes clearly more diffusive upon the KI intercalation as we compare Figs. 3(a)–3(c). We calculate the electron distribution change upon the intercalation by subtracting the sum of the electron densities of KI chain and (10,10) CNT from that of KI@(10,10) CNT, and then separate the increasing and decreasing portions of the density. We plot the increasing and decreasing portions of the electron density in Figs. 3(d) and 3(e), respectively. The induced density upon the intercalation is 10%–30% of the original density, which is significant and indicates the strong interaction between the KI chain and the tube wall. The area encircled by the gray dashed lines depicts the atomic spheres used in the LAPW method, and the rest is the interstitial region defined as such. The radii for carbon, potassium, and iodine in this case are 1.30, 3.00, and 3.80, respectively, as indicated in Fig. 3(f). In Figs. 3(d) and 3(e), we found that the induced electron densities near potassium and iodine are confined within the atomic spheres. The decreased density within I atomic spheres is much larger than the increased portion, and this implies that the electrons may transfer from the KI chain to the wall. The increasing portion of the density is most around the wall, as shown in Fig. 3(d), while the decreasing portion is most within the atomic spheres (as defined by the LAPW method) of carbon atoms on the wall or the I atoms inside the tube. All these are consistent with our prior observation that electrons diffuse

TABLE I. Charge distributions in KI@(10,10) CNT, (10,10) CNT, and KI chain[a]

| | Number of electrons within the cell | | |
|---|---|---|---|
| Region | KI@(10,10) | (10,10) | KI |
| $C_{120}$ | 401.73 | 436.48 | ··· |
| $K_4I_4$ | 281.53 | ··· | 282.53 |
| Interstitial | 324.74 | 283.52 | 5.47 |

[a]Radii of carbon, potassium, and iodine atomic spheres are 1.30, 3.00, and 3.80 a.u., respectively.

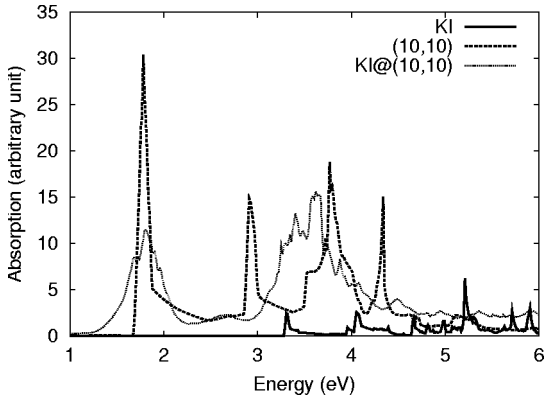


FIG. 4. Absorption spectrum of KI@(10,10), (10,10) CNT, and KI. The solid line is for the KI chain, the dashed line is for (10,10) CNT, and the dotted line is for KI@(10,10) CNT.

from the highly dense LAPW atomic spheres to the LAPW interstitial region.

To quantify the charge transfer, we calculate the number of electrons inside the LAPW atomic spheres and within the LAPW interstitial region. Table I shows the charges in the atomic spheres and interstitial regions of KI@(10,10) nanotube, (10,10) nanotube, and linear chain KI. In the calculation of the KI chain, we use the same unit cell as KI@(10,10) CNT by removing carbon atoms. The results show that there is a substantial amount of electron transfer from the carbon atomic spheres into the interstitial region upon the KI intercalation. The sum of the numbers of electrons in the LAPW interstitial regions of separate KI and (10,10) CNT are 288.99, while that of KI@(10,10) CNT is increased to 324.74. There are 0.3 electrons per carbon atom transferred from its LAPW atomic sphere region to the LAPW interstitial region of the tube, and one electron transfers from every four KI LAPW atomic spheres to the LAPW interstitial region. Calculations have been carried out for different muffin-tin radii of potassium and iodine, and the result remains that one electron transfers from K and I atomic spheres to the interstitial region within a unit cell. All these confirm that one out of every four K 4*s* electrons transfers to the tube wall upon the KI intercalation, while the other three go to I 5*p* orbitals as expected. Jhi *et al.* performed pseudopotential DFT calculation on bromine intercalated nanotubes,[13] and found that electrons transfer to bromine. In our case, 75% of K 4*s* electrons transfer to iodine, while the rest goes to the vicinity of the tube wall.

It is found that the optical properties of CNTs are strongly affected by the tube length, radius, end group, chirality, and bond length.[14] In this work, the effect of KI intercalation on the optical properties of CNT is presented. Figure 4 shows the calculated absorption spectra of KI@(10,10) CNT, (10,10) CNT, and KI chain. The absorption spectrum of KI@(10,10) tube is not a simple sum of those of the (10,10) tube and KI chain. This supports further the existence of a strong interaction between the KI chain and the tube wall. It is observed that the peak at about 1.8 eV broadens considerably upon the intercalation. This is consistent with our calculation that the DOS changes near the Fermi level upon the KI intercalation, as indicated by the insets of Fig. 2. Significant energy shifts are observed for the absorption bands beyond the first band.

To summarize, we have investigated the electronic structure of potassium iodide intercalated CNTs using a first-principles DFT calculation. Upon the intercalation, the electrons on the tube become much more diffused, which indicates the strong interaction between KI and the tube wall. The strong interaction alters the electronic structures and the DOS near the Fermi level. Moreover, one out of every four K 4*s* electrons transfers to the tube wall upon the intercalation.

Support from the Hong Kong Research Grant Council (RGC) and the Committee for Research and Conference Grants (CRCG) of the University of Hong Kong is gratefully acknowledged.

[1] S. Iijima, Nature (London) **354**, 56 (1991).
[2] R. Saito, G. Dresselhaus, and M. S. Dresselhaus, *Physical Properties of Carbon Nanotubes* (Imperial College Press, London, 1998).
[3] T. W. Odom, J. L. Huang, P. Kim, and C. M. Lieber, Nature (London) **391**, 62 (1998).
[4] R. S. Lee, H. J. Kim, J. E. Fischer, A. Thess, and R. E. Smalley, Nature (London) **388**, 255 (1997).
[5] B. W. Smith, M. Monthioux, and D. E. Luzzi, Nature (London) **396**, 323 (1998).
[6] T. Miyake and S. Saito, Phys. Rev. B **65**, 165419 (2002).
[7] S. Okada, S. Saito, and A. Oshiyama, Phys. Rev. Lett. **86**, 3835 (2001).
[8] J. Sloan, M. C. Novotny, S. R. Bailey, G. Brown, C. Xu, V. C. Williams, S. Friedrichs, E. Flahaut, R. L. Callender, A. P. E. York, K. S. Coleman, M. L. H. Green, R. E. Dunin-Borkowski, and J. L. Hutchison, Chem. Phys. Lett. **329**, 61 (2000).
[9] R. R. Meyer, J. Sloan, R. E. Dunin-Borkowski, A. I. Kirkland, M. C. Novotny, S. R. Bailey, J. L. Hutchison, and M. L. H. Green, Science **289**, 1324 (2000).
[10] W. Kohn and L. J. Sham, Phys. Rev. **140**, A1133 (1965).
[11] P. Blaha, K. Schwarz, and J. Luitz, WIEN97, *A Full Potential Linearized Augmented Plane Wave Package for Calculating Crystal Properties* (Karlheinz Schwarz, Techn. Universitat Wien, Austria, 1999).
[12] J. P. Perdew and Y. Wang, Phys. Rev. B **45**, 13244 (1992).
[13] S. H. Jhi, S. G. Louie, and M. L. Cohen, Solid State Commun. **123**, 495 (2002).
[14] W. Z. Liang, X. J. Wang, S. Yokojima, and G. H. Chen, J. Am. Chem. Soc. **122**, 11129 (2000); W. Z. Liang, S. Yokojima, M. F. Ng, G. H. Chen, and G. Z. He, *ibid.* **123**, 9830 (2000).